Low E Modulus Early Strength Engineered Cementitious Composites Material

Development for Ultrathin Whitetopping Overlay

Zhigang Zhang, Qian Zhang, Shunzhi Qian, and Victor C. Li

For a reliable repair solution to be provided for the sinkage of concrete pavement slabs caused by the subsidence of subgrade, low E modulus early strength high ductility engineered cementitious composites (LMES-ECC) material was developed for ultrathin whitetopping overlay application. Low modulus of the topping material is advantageous for deformation compatibility with the existing substrate concrete without the experience of high stress. The high tensile ductility of LMES-ECC further increases the deformation compatibility and suppresses the reflective cracking, which is a major failure mechanism of pavement repair. Experimental studies were conducted on LMES-ECC with respect to its compressive strength, tensile properties, cracking behavior under restrained shrinkage, and flexural properties. The compressive strength and flexural strength of LMES-ECC at 3 days reached 31 MPa and 7 MPa, respectively, which satisfied both the requirement necessary to reopen traffic and the design strength of concrete pavement material. Unlike the brittle fracture of normal concrete, multiple microcracks (i.e., average crack width below 60 μm) developed in LMES-ECC before final fracture under tension and bending; this deformation resulted in a tensile strain capacity as high as 4% (about 400 times that of normal concrete) and large vertical deflection capacity. In addition, the E modulus of LMES-ECC was measured at 14 GPa, which was significantly lower than for normal concrete. The low modulus and high deformation capacity of LMES-ECC greatly improved the deformation compatibility of the topping overlay with the old concrete substrate, avoided brittle failure or large cracks of the overlay, and contributed to more effective pavement repair.

Subsidence of pavement slab caused by the sinkage of the subgrade has been identified as one of the major problems currently associated with cement concrete pavement in China. In the past decade, a large amount of cement concrete pavement has been constructed in China. With the rapid growth of the economy, the volume of transportation has increased sharply in recent years. The subsidence of pavement slab as a result of subgrade sinkage has become prevalent as a result of the increasing traffic load. Because of soft ground and roadbed fill materials, sinkage of subgrade is commonly found in bridge head and high fill subgrade construction. Such sinkage will not cause structural failure of the pavement on top of it. However, it does have negative impacts on driving comfort and driving safety.

A common way to solve this problem is to crush the original pavement and produce new asphalt or cement concrete pavement to achieve the original design elevation. However, this solution is costly and has adverse environmental impacts, because the crushed original pavement material needs to be disposed of. As a way to reuse the original cement concrete pavement, the introduction on top of it of an ultrathin overlay with cement concrete or asphalt has been investigated by many researchers as an alternative solution (*1, 2*).

Ultrathin whitetopping overlay, which refers to cement concrete overlay, is considered more sustainable and cost effective than asphalt overlay. Asphalt overlay offers many advantages, such as surface smoothness, jointless connection, low noise, driving comfort, and easy maintenance. However, the disadvantages of asphalt overlay also are pronounced. They include strong temperature sensitivity, low resistance to water damage, low shear resistance, and high construction costs (*3–5*). The asphalt pavement construction process also is pollution intensive. A cement concrete topping overlay, with its higher resistance to water and temperature damage, has a much longer service life than does an asphalt topping overlay. Thus it requires less maintenance. Given the cost of a topping overlay with respect to the entire service life and the environmental impact, cement concrete is potentially a better option for the ultrathin topping overlay application.

Although more sustainable and durable than asphalt, the durability of ultrathin whitetopping overlay is still limited by the quasi-brittle and crack-prone nature of cement concrete. Unlike new pavement, the durability of the ultrathin whitetopping overlay depends greatly on the compatibility between the new topping overlay material and the existing substrate concrete (*6*). For ultrathin whitetopping overlay made of conventional cement concrete materials, cracks can form easily because of incompatible deformation (e.g., deformation caused by shrinkage of the topping overlay) between the overlay and the substrate concrete pavement. As a result, debonding between the overlay and concrete substrate often is observed (*7*). Another main failure mechanism for ultrathin topping overlay made of conventional cement concrete is so-called reflective cracking. Reflective cracking refers to the phenomenon in which existing cracks in the substrate concrete pavement are reflected to the new topping overlay (*8–12*). The cracking of the conventional cement concrete topping overlay increases water permeability and chloride penetration, which contributes to accelerated deterioration of the overlay system and thus limits the service life and requires frequent repairs (*7*). Up to half of all concrete repairs prematurely fail, which leads to frequent maintenance

Z. Zhang, Institute of Highway and Railway Engineering, School of Transportation, Southeast University, Nanjing 210096, China. Q. Zhang and V. C. Li, Department of Civil and Environmental Engineering, University of Michigan, 2350 Hayward Street, Ann Arbor, MI 48109-2125. S. Qian, Department of Civil and Environmental Engineering, Nanyang Technological University, Singapore 639798. Corresponding author: V. C. Li, vcli@umich.edu.

Transportation Research Record: Journal of the Transportation Research Board, No. 2481, Transportation Research Board, Washington, D.C., 2015, pp. 41–47.
DOI: 10.3141/2481-06

and repair throughout the service life and results in significant life-cycle economic, social, and environmental impacts (*13*).

To enhance the durability of the ulrathin whitetopping overlay, to avoid reflective cracking, and to ensure deformation compatibility with the existing concrete, material with high tensile ductility and equal or lower elastic modulus than that of the substrate concrete pavement is desired for the topping overlay.

In this study, engineered cementitious composites (ECC), a type of high-performance fiber-reinforced cementitious composites, was introduced into the ultrathin whitetopping overlay application. ECC material has been developed by Li on the basis of micromechanical theory over the past decade (*14*). ECC, with less than 2% (by total volume) of polymer fiber, achieves a tensile strain capacity that ranges between 3% and 5%, which is about 300 to 500 times the capacity of conventional concrete (*15, 16*). Unlike brittle fracture failure commonly observed in normal concrete, multiple fine cracks (typically below 100 μm in width) develop in ECC under tension before final fracture, which results in a metal-like strain-hardening behavior with significantly higher tensile strain capacity. ECC with high tensile ductility, as discussed, could be a plausible solution to enhance the durability of ultrathin whitetopping overlay.

The freeze–thaw durability and traffic wear resistance of ECC also were demonstrated to be sufficient for pavement application according to previous studies. The resistance of ECC to freeze–thaw cycles was shown to be superior to that of normal concrete. During the freeze–thaw test, ECC specimens without air-entrainment survived and retained high ductility even after 300 test cycles, while normal concrete without air entrainment failed after only 100 cycles (*17, 18*). The surface friction and wear track test on ECC specimens was conducted by the Michigan Department of Transportation in 2003. The aggregate wear index, which refers to the final friction force after 4 million tire passes, was measured to be 1.6 to 2.3 kN for textured ECC specimens, well above the established requirement for Michigan trunk line road surfaces at 1.2 kN (*18*). On the basis of these test results, ECC was considered a suitable material for pavement applications.

ECC showed great cost effectiveness when whole life-cycle cost was considered. The initial cost of ECC material is two to three times that of normal concrete. However, because of its significantly higher durability, ECC, as pavement material, has much longer service life and requires less maintenance during the entire service life. Thus the life-cycle cost of ECC in practice is estimated to be 30% to 40% less than that of the conventional pavement materials (*19*). In addition to cost-effectiveness, the successful field applications of ECC in Japan and the United States further demonstrated its advantages and provided guidance for future application of ECC in transportation infrastructure (*18*).

Besides high tensile ductility, specific features including high early strength and low Young's modulus also are preferred for cement concrete topping overlay application. During pavement repair, normal highway operation is disrupted. Traffic congestion during construction can increase energy consumption and greenhouse gas emissions significantly (*20*). To minimize these impacts, early strength material that allows fast construction is preferred. In China, it is typically required that a road be reopened to traffic in 3 days, which puts a stringent requirement on the early strength of the topping overlay material. In addition to early strength, a low elastic modulus is desirable because it lowers the tensile stress buildup from restrained shrinkage (*21*). The result is a reduction in the cracking tendency of the topping overlay and a reduction in the magnitude of delamination at the overlay–substrate interface. For the reasons discussed here, it was determined that low E modulus early strength high ductility engineered cementitious composites (LMES-ECC) material was needed for durable topping overlay applications. Although LMES and high early strength ECCs have been developed in previous research, they have never been developed simultaneously in one ECC material (*22, 23*).

In this study, LMES-ECC material was developed for durable ultrathin whitetopping overlay application. The compressive strength, tensile and flexural behavior, crack pattern, E modulus, and restrained shrinkage behavior of LMES-ECC were investigated. The evolution of mechanical behavior over curing age was studied also. All investigation procedures and test results are documented in this paper.

EXPERIMENTAL PROGRAMS

Materials and Mix Proportions

In this study, ingredients including Type 3 portland cement, fly ash, silica sand, crumb rubber, water, polyvinyl alcohol (PVA) fiber, nonchloride accelerator, and polycarboxylate-based high water reducer were used in the production of LMES-ECC mixture. Type 3 portland cement and accelerator were used to achieve early strength, and crumb rubber was used to reduce the E modulus of the mixture. The crumb rubber used in this study is shown in Figure 1. The size of the crumb rubber particles was 40 CR, which meant the particles could pass Sieve No. 40 (with a sieve opening of 420 μm). The density of crumb rubber and silica sand was 1.2 g/cm^3 and 2.6 g/cm^3, respectively. The geometrical and mechanical properties of PVA fiber are as follows:

- Diameter = 39 μm,
- Length = 12 mm,
- Tensile strength = 1,600 MPa,
- Modulus = 42 GPa, and
- Density = 1.3 g/cm^3.

The mix proportion of LMES-ECC is as follows:

- Cement = 420 g/L,
- Fly ash = 841 g/L,

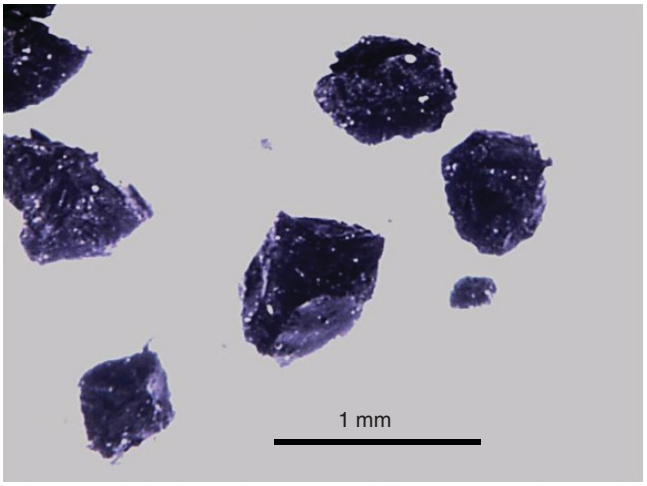

FIGURE 1 Crumb rubber.

- Sand = 344 g/L,
- Crumb rubber = 53 g/L,
- Water = 312 g/L,
- High water reducer = 6 g/L,
- Accelerator = 31 g/L, and
- PVA = 26 g/L.

A LMES-ECC mixture with a water–binder ratio of 0.25, fly ash–cement ratio of 2.0, and 4.5% (by volume fraction) of crumb rubber was used in this study.

The LMES-ECC mixture was mixed according to a standard ECC mixing procedure. All solid ingredients including cement, fly ash, silica sand, and crumb rubber were mixed dry for 3 min. Water, high water reducer, and accelerator agent were then added to the dry mixture and mixed for another 3 min. PVA fiber was slowly added into the mortar and mixed for 5 min until fibers were well dispersed. To simulate the curing condition in the construction field, the fresh LMES-ECC (except for what was used in the restrained shrinkage ring test) was then cast into molds covered with plastic sheets. The specimens were demolded after 1 day of curing, and the plastic sheets were removed after 3 days. The specimens were then cured at an air room temperature of 20°C ± 3°C (68°F ± 5°F) and a relative humidity of 40% ± 5%.

Specimen Preparation and Testing

Compressive strength of LMES-ECC was measured with a set of three cube specimens whose dimensions were 50.8 × 50.8 × 50.8 mm in accordance with ASTM C109.

Uniaxial tensile tests were conducted to characterize the tensile performance of LMES-ECC at different curing ages in accordance with the Japan Society of Civil Engineers recommendation for design and construction of high-performance fiber-reinforced cement composites with multiple fine cracks (*24*). Four sets of dog bone–shaped specimens (three specimens in each set) were tested at 1, 3, 7, and 28 days, respectively. The detailed dimensions of the specimens and the configurations of the uniaxial tensile test setup are found in Figure 2.

A four-point bending test was used to evaluate the bending deformation capacity of LMES-ECC. The test was conducted under a quasi-static loading condition with deformation control of 0.5 mm per minute at loading points. The full span length of the bending test was 300 mm with a middle span of 100 mm. During the test, the load and loading point displacement were recorded. Four sets of specimens (three specimens in each set) were tested at 3, 7, 14, and 28 days, respectively.

For a better understanding of the multiple cracking behavior, the crack width and crack number of the tensile test specimens were measured after unloading. A portable microscope was used with a precision of 10 μm.

A restrained shrinkage ring test was used to evaluate the cracking behavior of ECC mixtures under restrained shrinkage conditions, which form a critical property for concrete repairs. A layer of ECC mixture 25.4-mm thick was cast around a rigid steel ring with a height of 152.4 mm and inner and outer diameters of 304.8 and 355.5 mm, respectively. A detailed description of the restrained ring test setup can be found in Keoleian et al. (*20*). After casting, the top surface of fresh ECC was sealed by epoxy resin immediately. The ring specimens were cured for 24 h before removal of the mold on the outer surface of the specimen. The specimens were then exposed to an air temperature of 23°C ± 3°C and a relative humidity of 25% ± 5%. A uniform radial pressure was exerted on the steel ring as a result of the shrinkage of ECC, which in turn induced tensile hoop stresses and subsequent cracking on the ECC mortar specimens. Crack widths, numbers, and length were measured with a portable

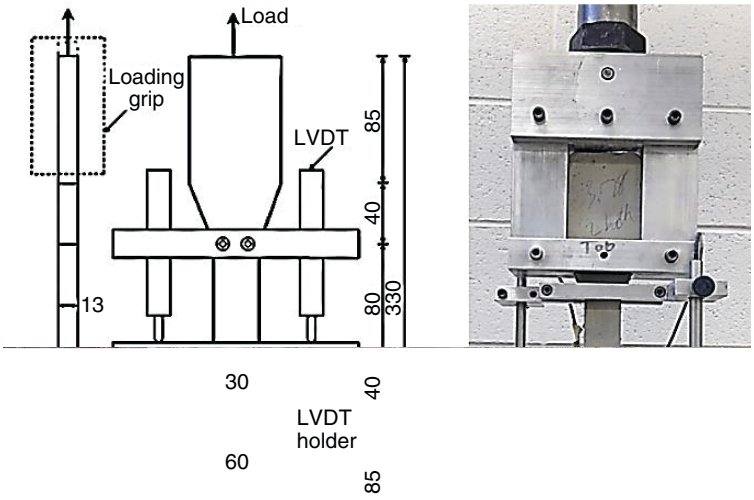

FIGURE 2 Dimension of dog-bone specimen and tensile test setup (LVDT = linear variable differential transformer).

microscope and a ruler, whose respective accuracies were 10 μm and 1 mm.

RESULTS AND DISCUSSIONS

Compressive Strength of LMES-ECC

In normal pavement material design, the designed compressive strength of concrete material should not be lower than 36 MPa for a road that carries moderate traffic. Once the compressive strength is 70% of the designed compressive strength (i.e., no lower than 25 MPa) the road can be opened to traffic (Chinese standard JTJ-037). This requirement could be used as a standard to evaluate the effectiveness of LMES-ECC for fast repair. The compressive strengths of LMES-ECC at different curing ages were plotted in Figure 3. Specimens were tested at 1, 2, 3, 7, 14, and 28 days. The compressive strength increased sharply at an early age; it reached 31 MPa in 3 curing days, which meant the road could be reopened to traffic 3 days after casting with the use of the early strength ECC material developed in this study. The strength development slowed after 7 days. After 28 days of curing, the compressive strength of LMES-ECC reached 43 MPa, which well satisfied the strength requirement for pavement material (Chinese standard JTG-D40).

Tensile Properties of LMES-ECC

The representative tensile stress–strain curves for LMES-ECC at different curing ages are presented in Figure 4. These curves can be divided into two stages. First, LMES-ECC undergoes elastic strain under tension before the first microcrack appears. Then it enters into the strain-hardening stage accompanied by multiple microcrack development. The slope of the elastic stage is determined as elastic modulus under tension. The strain that corresponds to the maximum tensile stress is defined as tensile strain capacity.

Unlike the brittle fracture of normal concrete under tension, LMES-ECC exhibited a ductile damage pattern. The crack width of LMES-ECC was below 80 μm; the number of cracks continued to increase before the saturated cracking state was reached. The fibers that bridged the crack surfaces continued to carry increasing stress before a localized fracture occurred as a result of the exhaustion of

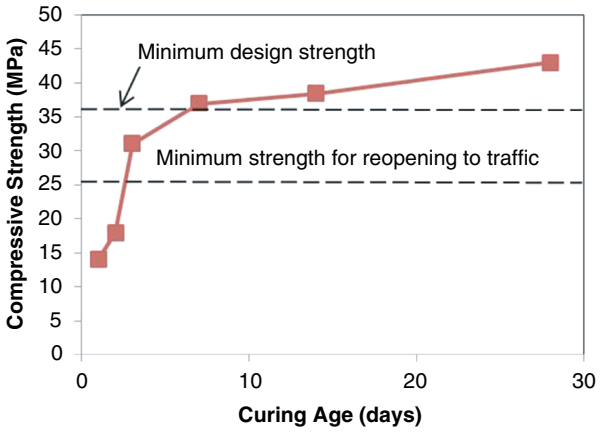

FIGURE 3 Compressive strength development of LMES-ECC with curing ages.

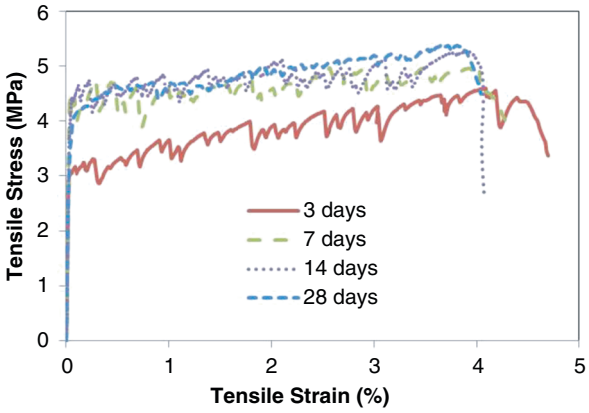

FIGURE 4 Tensile property of early strength ECC at different curing days.

the fiber's bridging capacity. Thus a pseudo strain-hardening behavior was achieved with a substantially higher strain capacity.

As shown in Figure 4, the tensile strain of ECC at all curing ages could reach 4%, about 400 times that of normal concrete with approximately 0.01% tensile strain. LMES-ECC maintained about the same level of tensile ductility as the curing age increased up to 28 days. After 3 days of curing, the tensile strength was 4.5 MPa, and it gradually increased to 5.3 MPa at 28 days. The increase in ECC tensile strength with curing age resulted from the further hydration of the matrix and the development of interface bonding between the fiber and matrix.

Crack information, including crack number, average crack width, and crack pattern, is presented in Table 1 and Figure 5. As shown in Figure 5, the crack number increased with curing age, while the spacing between adjacent microcracks decreased. Table 1 shows that the average crack width decreased from 56 to 16 μm as the curing age increased from 3 to 28 days because of the change in fiber bridging behavior during curing. With such fine cracks in ECC, the water permeability coefficient and chloride diffusion property were found to be nearly the same as those of uncracked concrete (*25, 26*). Thus the microcrack pattern in ECC was expected to have little impact on water transport property and durability.

The measured E modulus of LMES-ECC under tension at different curing ages is as follows:

- 3 days = 14.6 ± 0.9 GPa,
- 7 days = 14.4 ± 0.3 GPa,
- 14 days = 14.4 ± 0.6 GPa, and
- 28 days = 14.4 ± 0.5 GPa

As the table shows, the E modulus of LMES-ECC was independent of curing age, with little change after 3 days. The E modulus

TABLE 1 Crack Information on LMES-ECC After Tensile Test

Curing Age (days)	Crack Number	Average Crack Width (μm)	Maximum Crack Width (μm)
3	40	56	80
7	65	22	50
14	61	21	40
28	75	16	40

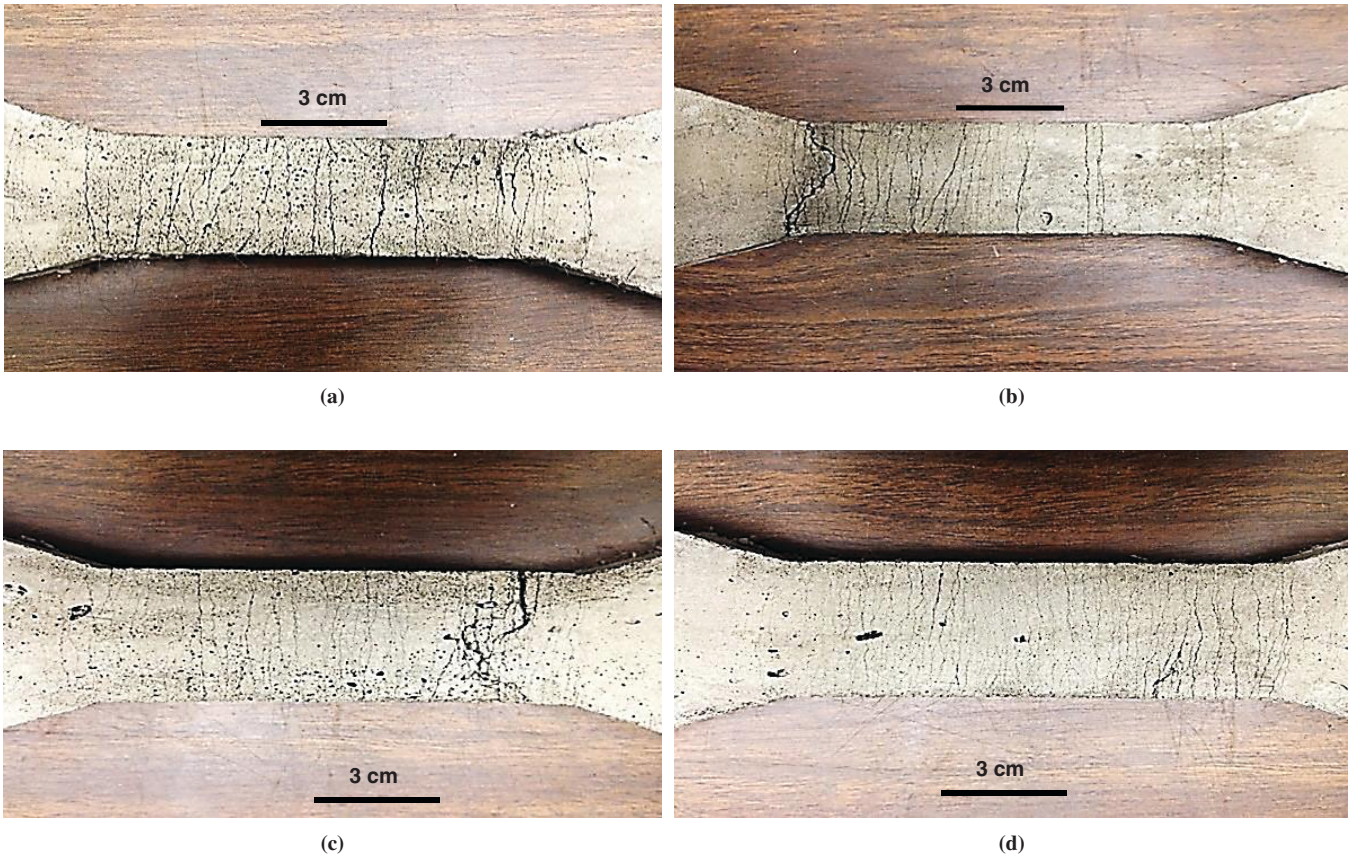

FIGURE 5 Observed crack patterns in LMES-ECC specimens after tensile test: (*a*) 3 days, (*b*) 7 days, (*c*) 14 days, and (*d*) 28 days.

of LMES-ECC was 14.4 GPa at 28 days, which was lower than that of normal concrete (typically 30 GPa). The low E modulus could be attributed to the combined effects of the absence of coarse aggregate and the incorporation of crumb rubber (*23*).

For investigation of cracking behavior under a restrained tension condition, a restrained shrinkage ring test was used in this study. Table 2 shows the cracking behavior of LMES-ECC in detail. Unlike normal concrete, there was no localized fracture for the LMES-ECC ring specimen during the testing period. Only very tight cracks could be observed on the specimen surface. Similarly to the tensile test, the crack number and total crack length increased from 3 to 14 days, while crack width decreased. After 14 days and until 28 days, the cracking state remained unchanged. The final crack width was tight (below 40 μm), which had little impact on the durability compared with the millimeter-sized cracks typically found in conventional concrete.

TABLE 2 Cracking Behavior of LMES-ECC Under Restrained Shrinkage

Curing Age (days)	Crack Number	Crack Length (mm)	Average Crack Width (μm)
3	3	334	38
14	7	841	24
28	7	841	24

Flexural Properties of LMES-ECC

Apart from compressive strength, the flexural strength of pavement repair material usually is specified as an important parameter with respect to the reopening of a roadway to traffic. According to the standard of concrete pavement maintenance technology in China, the designed flexural strength of pavement material is required to be no lower than 5 MPa, while a minimum flexural strength of 3.5 MPa is required before a highway can be reopened to traffic.

Figure 6 exhibits the representative flexural stress load point displacement curves for LMES-ECC at 3, 7, 14, and 28 days. The maximum flexural stress is defined as flexural strength, while the corresponding displacement is defined as flexural deflection capacity.

The flexural strength of LMES-ECC at 3 days could reach 7 MPa, which satisfied the requirement with respect to the reopening of a road to traffic, and it even exceeded the required design flexural strength of pavement material. The flexural strength reached 9.5 MPa at 28 days. Similar to the tensile stress–strain curve, after a linear elastic stage at the beginning, the curve entered a deflection hardening stage: the flexural stress increased at a slow rate as the loading point displacement increased, accompanied by multiple microcracks that developed along the specimen length. Figure 7 shows the typical cracking pattern of ECC. During the flexural test on LMES-ECC, the first crack started inside the midspan at the tensile surface, and then multiple cracks with tiny crack widths developed within the midspan and gradually expanded to the outside of the midspan. This behavior was different from that of conventional concrete, which typically forms a single, localized crack and fails in brittle fracture. The deflection

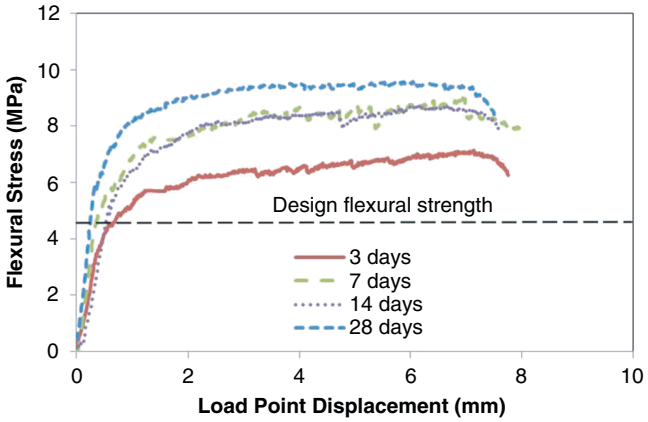

FIGURE 6 LMES-ECC flexural stress–displacement curves at different ages.

capacity of LMES-ECC remained almost at a constant level as the curing age increased. During a four-point bending test, the load point displacement reached 7 mm, which was much more than normal concrete reached with no inelastic deformation capacity. With the large deflection capacity, the topping overlay could accommodate the vertical deformation of substrate concrete when subject to traffic load.

CONCLUSIONS

In this study, LMES-ECC was developed as an ultrathin whitetopping overlay. On the basis of the experimental results of this study, the following conclusions were drawn:

1. The compressive strength of LMES-ECC reached 31 and 43 MPa at 3 and 28 days, respectively. This result meant that a road could be reopened to traffic 3 days after casting, which satisfied the requirement for fast repair. The compressive strength of LMES-ECC at 28 days also satisfied the requirement of pavement material for heavy traffic.
2. The tensile strain capacity of LMES-ECC was 4%, which was about 400 times that of normal concrete. Under tension, multiple microcracks (with an average crack width below 60 μm) developed in LMES-ECC, unlike the localized fracture cracks that occur in normal concrete, and the tight crack width had much less impact on the durability of the overlay system.
3. The E modulus of LMES-ECC under tension was about 14 GPa, which was much lower than that of normal concrete and regular ECC material. Such a low modulus could lower the induced tensile stress buildup caused by restrained shrinkage.
4. The flexural strength of LMES-ECC at 3 days reached 7 MPa, which satisfied the requirement to reopen a road to traffic. This value exceeded the required design flexural strength of pavement material. The deflection capacity of LMES-ECC was above 7 mm at all ages, an indication of a much higher vertical deformation capacity than the substrate concrete, and allowed it to fully accommodate the vertical deformation of substrate concrete when subject to traffic load.

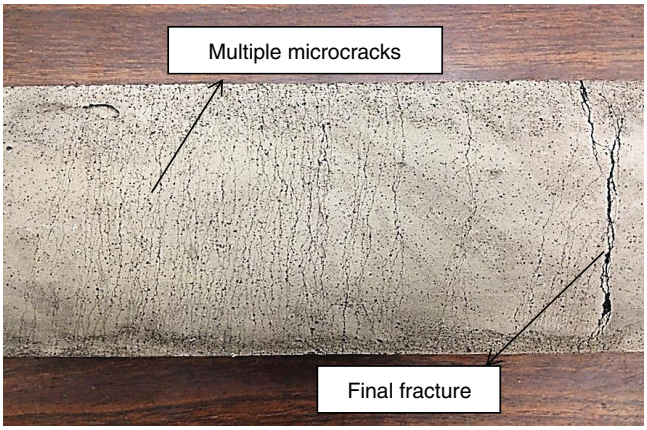

FIGURE 7 Typical crack patterns in LMES-ECC specimens after bending test.

In this study, LMES-ECC material with high tensile ductility was developed for an ultrathin whitetopping overlay application. This preliminary experimental study on the material's behavior is presented in this paper. However, before field application, further investigation is needed, including large-scale testing, detailed design of the overlay, and consideration of possible alternative mixtures.

ACKNOWLEDGMENTS

The first author was supported by a grant from the Chinese Scholarship Council as a visiting scholar at the University of Michigan, Ann Arbor. The authors thank the Holcim Company, the Boral Company, U.S. Silica, Kuraray Company, and W.R. Grace & Company for their respective provision of Type 3 ordinary portland cement, fine silica sand, Class F normal fly ash, PVA fibers, high-range water-reducing admixture, and accelerator agent.

REFERENCES

1. Speakman, J., and H.N. Scott III. Ultra-Thin, Fiber-Reinforced Overlays for Urban Intersections. In *Transportation Research Record 1532,* TRB, National Research Council, Washington, D.C., 1996, pp. 15–20.
2. Rotithor, H.G. *Performance of Ultrathin White Topping in Oklahoma.* PhD dissertation, Oklahoma State University, Stillwater, 2011.
3. Fwa, T.F., S.A. Tan, and L.Y. Zhu. Rutting Prediction of Asphalt Pavement Layer Using C-ϕ Model. *Journal of Transportation Engineering,* Vol. 130, No. 5, 2004, pp. 675–683.
4. Castillo, D., and C. Silvia. Effects of Air Voids Variability on the Thermomechanical Response of Asphalt Mixtures. *International Journal of Pavement Engineering,* Vol. 15, No. 2, 2014, pp. 110–121.
5. Hicks, R.G., L. Santucci, and T. Aschenbrener. Introduction and Seminar Objectives. *Proc., Moisture Sensitivity of Asphalt Pavements: A National Seminar.* San Diego, Calif., Transportation Research Board of the National Academies, Washington, D.C., 2003, pp. 3–20.
6. Morgan, D.R. Compatibility of Concrete Repair Materials and Systems. *Construction and Building Materials,* Vol. 10, No. 1, 1996, pp. 57–67.
7. Emmons, P.H., and D.J. Sordyl. The State of the Concrete Repair Industry, and a Vision for Its Future. *Concrete Repair Bulletin,* July–Aug. 2006, pp. 7–14.
8. Czarnecki, L., A. Garbacz, P. Lukowski, and J.R. Clifton. *Polymer Composites for Repairing Portland Cement Concrete: Compatibility Project.* Technical Report NISTIR 6394. National Institute of Standards and Technology, Gaithersburg, Md., 1999.
9. Emmons, P.H., A.M. Vaysburd, R.W. Poston, and J.E. McDonald. *Performance Criteria for Concrete Repair Materials,* Phase II, Field Studies. Technical Report REMR-CS-60. U.S. Army Waterways Experiment Station, Vicksburg, Miss., 1998.

10. Pigeon, M., and B. Bissonnette. Bonded Concrete Repairs: Tensile Creep and Cracking Potential. *Concrete International,* Vol. 21, No. 11, 1999, pp. 31–35.
11. Vaysburd, A. M. *Research Needs for Establishing Material Properties to Minimize Cracking in Concrete Repairs.* Summary of a Workshop. International Concrete Repair Institute Publication No. Y320001. National Institute of Standards and Technology, Gaithersburg, Md., 1996.
12. Huang, Y. H. *Pavement Analysis and Design,* 2nd ed. Prentice Hall, Upper Saddle River, N.J., 2003.
13. Vaysburd, A. M., C. D. Brown, B. Bissonnette, and P. H. Emmons. Realcrete Versus Labcrete. *Concrete International,* Vol. 26, No. 2, 2004, pp. 90–94.
14. Li, V. C. From Micromechanics to Structural Engineering: Design of Cementitious Composites for Civil Engineering Applications. *Journal of Structural Mechanics and Earthquake Engineering,* Vol. 10, No. 2, 1993, pp. 37–48.
15. Li, V. C. Engineered Cementitious Composites: Tailored Composites Through Micromechanical Modeling. In *Fiber Reinforced Concrete: Present and the Future* (N. Banthia, A. Bentur, and A. Mufti, eds.), Canadian Society for Civil Engineering, Montreal, Quebec, Canada, 1998, pp. 64–97.
16. Li, V. C., C. Wu, S. Wang, A. Ogawa, and T. Saito. Interface Tailoring for Strain-Hardening Polyvinyl Alcohol-Engineered Cementitious Composite. *ACI Materials Journal,* Vol. 99, No. 5, 2002, pp. 463–472.
17. Sahmaran, M., M. Lachemi, and V. C. Li. Assessing the Durability of Engineered Cementitious Composites Under Freezing and Thawing Cycles. *Journal of ASTM International,* Vol. 6, No. 7, 2009, pp. 102406–102419.
18. Qian, S., and V. C. Li. Ductile Concrete-Engineered Cementitious Composites for Durable Bridge Deck Repair and Rehabilitation. Presented at 90th Annual Meeting of the Transportation Research Board, Washington, D.C., 2011.
19. Li, M., R. Ranade, L. Kan, and V. C. Li. On Improving the Infrastructure Service Life Using ECC to Mitigate Rebar Corrosion. *Proc., Second International Symposium on Service Life Design for Infrastructure,* Delft, Netherlands, RILEM, Bagneux, France, 2010.
20. Keoleian, G. A., A. Kendall, J. E. Dettling, V. M. Smith, R. F. Chandler, M. D. Lepech, and V. C. Li. Life Cycle Modeling of Concrete Bridge Design: Comparison of ECC Link Slabs and Conventional Steel Expansion Joints. *Journal of Infrastructure Systems,* Vol. 11, No. 1, 2005, pp. 51–60.
21. Li, M. *Multiscale Design for Durable Repair of Concrete Structures.* PhD dissertation. University of Michigan, Ann Arbor, 2009.
22. Li, M., and V. C. Li. High-Early-Strength Engineered Cementitious Composites for Fast, Durable Concrete Repair-Material Properties. *ACI Materials Journal,* Vol. 108, No. 1, 2011, pp. 3–12.
23. Huang, X., R. Ranade, W. Ni, and V. C. Li. On the Use of Recycled Tire Rubber to Develop Low E Modulus ECC for Durable Concrete Repairs. *Construction and Building Materials,* Vol. 46, 2013, pp. 134–141.
24. *Recommendations for Design and Construction of High Performance Fiber Reinforced Cement Composites with Multiple Fine Cracks.* Concrete Engineering Series 82. Japan Society of Civil Engineers, Tokyo, 2008.
25. Lepech, M. D., and V. C. Li. Water Permeability of Engineered Cementitious Composites. *Journal of Cement and Concrete Composites,* Vol. 31, No. 10, 2009, pp. 744–753.
26. Sahmaran, M., M. Li, and V. C. Li. Transport Properties of Engineered Cementitious Composites Under Chloride Exposure. *ACI Materials Journal,* Vol. 104, No. 6, 2007, pp. 604–611.

The Standing Committee on Pavement Preservation peer-reviewed this paper.